Jurnal Teknik Informatika (JUTIF)
P-ISSN: 2723-3863
E-ISSN: 2723-3871
Vol. 7, No. 1, February 2026, Page. 373-390
https://jutif.if.unsoed.ac.id
DOI: https://doi.org/10.52436/1.jutif.2026.7.2.5485

Hybrid LSTM Forecasting Framework with Mutual Information and PSO–GWO Optimization for Short-Term SARS-CoV-2 Prediction in Indonesia

Faulinda Ely Nastiti*[1], Shahrulniza Musa[2], Imam Riadi[3]

[1]Department of Information System,Universitas Duta Bangsa Surakarta, Surakarta, Indonesia
[2]Malaysian Institute of Information Technology, Universiti Kuala Lumpur, Kuala Lumpur, Malaysia
[3]Department of Information System, Universitas Ahmad Dahlan, Yogyakarta, Indonesia

Email: [1]faulinda_ely@udb.ac.id

Received : Nov 27, 2025; Revised : Dec 6, 2025; Accepted : Dec 6, 2025; Published : Feb 15, 2026

ABSTRACT

SARS-CoV-2 remains an endemic challenge in Indonesia, requiring reliable short-term forecasting tools that support informatics, digital epidemiology, and data-driven public health systems. Standard LSTM models, while widely used for epidemic forecasting, face notable limitations such as sensitivity to poor weight initialization, and reduced ability to capture interactions within heterogeneous high-dimensional data—resulting in inconsistent performance. This research introduces ADELMI (Adaptive Deep Learning Metaheuristic Intelligence), a unified hybrid forecasting framework specifically designed not only to enhance forecasting accuracy but also to overcome core weaknesses of traditional LSTM architectures when applied to complex epidemic datasets. ADELMI integrates Mutual Information and Pearson Correlation for dual feature selection with a hybrid Particle Swarm–Grey Wolf Optimization (PSO–GWO) approach for optimizing LSTM parameters. The dataset includes 657 daily observations and 82 epidemiological, vaccination, and meteorological variables sourced from the Ministry of Health and BMKG (2020–2021). Feature selection reduced the dataset to 20 relevant predictors for recovery and death and one dominant predictor for positive cases. The optimized 50-unit LSTM with early stopping achieved highly accurate 7-day forecasts, producing MAPE scores of 0.01% (positive cases), 1.44% (recoveries), and 3.00% (deaths) across 5-fold cross-validation. These results significantly outperform ARIMA, SIR, and baseline LSTM models. By unifying dual feature selection with hybrid PSO–GWO optimization, ADELMI improves LSTM stability, weight initialization, and multivariate interaction modeling, delivering more reliable forecasts across heterogeneous datasets. This advancement strengthens informatics through DL-metaheuristic multivariate epidemic modeling and enables proactive, adaptive surveillance against evolving threats such as influenza hybrids.

Keywords : *SAR-COV-2 Indonesia, deep learning hybrid, grey wolf optimization, long short-term memory, mutual information selection, particle swarm optimization*

1. INTRODUCTION

SARS-CoV-2, now in an endemic phase, continues to cause recurrent fluctuations in infections and mortality worldwide [1] [2]. Consequently, it is imperative for nations to establish dependable forecasting models for preparedness [3], given the persistent uncertainties regarding the virus's evolution and its effects on public health [4]. In response, researchers have prioritized developing accurate forecasting models to predict recovery, mortality, and infection rates [5], [6] in order to mitigate the pandemic's impact and guide policy decisions [7]. However, achieving reliable predictions remains a critical challenge due to the complex, nonlinear, and heterogeneous nature of virus datasets.

In Indonesia, diverse testing practices, varying vaccination progress, and heterogeneous meteorological patterns makes these challenges more complex than in Malaysia or Singapore [8], [9]. This unique multivariate landscape made conventional forecasting models unstable and underscores the

Vol. 7, No. 1, February 2026, Page. 373-390
https://jutif.if.unsoed.ac.id
DOI: https://doi.org/10.52436/1.jutif.2026.7.2.5485

need for a more adaptive and predictive framework tailored to Indonesian conditions. The limitations of classical epidemiological approaches further complicate short-term forecasting in Indonesia [10], [11].

Traditional approaches based on mathematical epidemiology, such as the Susceptible–Infectious–Removed (SIR) model and its derivatives, have been widely applied to capture infection dynamics [12]. Nonetheless, these deterministic models face major limitations in parameter estimation and adaptability, often resulting in inaccurate predictions under real-world outbreak conditions [13]. Consequently, research attention shifted toward machine learning and deep learning models capable of capturing nonlinear temporal dependencies and high-dimensional relationships. Milojkovic et al. [14], demonstrated that Artificial Neural Networks (ANN) achieved a Mean Absolute Error (MAE) of 5% in one-day-ahead predictions. Similarly, Kamarudin et al. [15], used a Multilayer Perceptron (MLP) model to obtain Root Mean Square Error (RMSE) values of 40.8, while Random Forest (RF) achieved an accuracy rate of 93.8% [16]. Prakash et al [17], hybridized the GRU with LSTM architecture achieved a RMSE 69.92 for positive cases prediction. Alkhalefah [5] evaluated the XGBoost-SIRVD-LSTM hybrid model and reported an RMSE of 35.025 and Mean Absolute Error (MAPE) of 0.9 for positive cases. Despite these improvements, most models struggled to maintain performance when faced with real and long-term epidemic data, as they are sensitive to data heterogeneity and noise [18].

The complexity of epidemic data lies in its heterogeneous–multivariable characteristics, encompassing diverse domains such as meteorology, demography, vaccination coverage, and population [19], [20]. These heterogeneous features evolve over time, increasing uncertainty and reducing the generalization of predictive models. To address this issue, feature selection methods have been employed to identify the most informative variables and improve computational efficiency. Several techniques, including Principal Component Analysis (PCA) [21], Genetic Algorithm (GA) [22], Pearson Correlation (PC) [23], and Neural Network–based selection [24] have demonstrated effectiveness in reducing irrelevant features. Mutual Information (MI) based feature selection, further advances this process by capturing nonlinear dependencies and statistical relationships between variables [25], while Pearson Correlation highlights linear associations that improve interpretability [26]. Together, these methods enable more efficient modeling of heterogeneous datasets and improve forecasting accuracy.

Deep learning models, especially Long Short-Term Memory (LSTM) networks, have demonstrated superiority in time-series forecasting tasks due to their ability to retain long-term temporal dependencies and capture complex patterns [27]. Previous studies indicate that LSTM consistently outperforms models such as ARIMA [10], [28], [29], RNN [30], [31], CNN [32], [33], and SVM [34] when applied to epidemic forecasting. However, the conventional LSTM model still faces critical weaknesses related to gradient instability, limited feature interaction modeling, and poor parameter initialization [35]. These limitations often hinder convergence and lead to suboptimal performance when processing large, heterogeneous datasets. To enhance model accuracy, researchers have incorporated metaheuristic optimization algorithms such as Particle Swarm Optimization (PSO) [36], [37], [38], Grey Wolf Optimizer (GWO) [39], [40], [41], and Genetic Algorithm (GA) [42] to tune model parameters. Although these single optimization methods have shown promise, they frequently become trapped in local optima, failing to fully explore the global search space.

Given these limitations, three major research gaps are identified. First, existing studies rarely integrate feature selection and model optimization in a unified framework, leading to inefficiencies in both data preparation and learning stages [21], [22], [23], [24], [25], [26], [43], [44]. Second, most predictive frameworks remain limited in their ability to manage heterogeneous–multivariable data dynamically, particularly when dealing with complex epidemic interactions influenced by diverse environmental and behavioral factors [18], [19], [20]. Third, optimization efforts using a single metaheuristic algorithm are prone to premature convergence, restricting adaptability in high-dimensional forecasting problems [39], [42], [45], [46].

To bridge these gaps, this research proposes ADELMI (Adaptive Deep Learning Metaheuristic Intelligence), a novel Hybrid Deep Learning Metaheuristics Intelligence Framework that integrates the strength of feature selection and hybrid optimization within an LSTM architecture. ADELMI employs

Vol. 7, No. 1, February 2026, Page. 373-390
https://jutif.if.unsoed.ac.id
DOI: https://doi.org/10.52436/1.jutif.2026.7.2.5485

Mutual Information and Pearson Correlation for dual feature selection to capture both nonlinear and linear relationships within the data. Subsequently, a hybrid Particle Swarm Optimization–Grey Wolf Optimizer (PSO–GWO) algorithm is used to optimize the parameters of the LSTM network. The hybridization of PSO and GWO enables global exploration and local exploitation simultaneously, reducing the risk of local minima and enhancing convergence stability. ADELMI enhances both forecasting precision and model generalization adaptable to endemic surveillance.

The novelty of this research lies in unifying dual feature selection and hybrid metaheuristic optimization into a single deep learning framework for short-term epidemic forecasting. Unlike existing works that focus on either optimization or feature extraction independently, this research bridges both aspects, producing a robust and computationally efficient model capable of adapting to evolving data conditions. This approach not only enhances predictive accuracy but also provides a methodological foundation applicable to future epidemic outbreaks and other domains involving multivariate time-series forecasting. The objective of this research was to evaluate the capability of the ADELMI framework in addressing heterogeneous epidemic data challenges and generating reliable 7-day forecasts for SARS-CoV-2 recovery, death, and positive cases.

2. METHOD

The research methodology is based on a post-positivist philosophical framework, acknowledging human cognitive [47] in understanding and predicting the spread of SARS-CoV-2. The research is conducted using quantitative methods for model prediction evaluation, to demonstrate that the ADELMI Framework has objectively accurate predictive capabilities This research involves experimental design using the Python programming language and TensorFlow library. To achieve the research objectives, the development of ADELMI predictive framework as depicted in Figure 1.

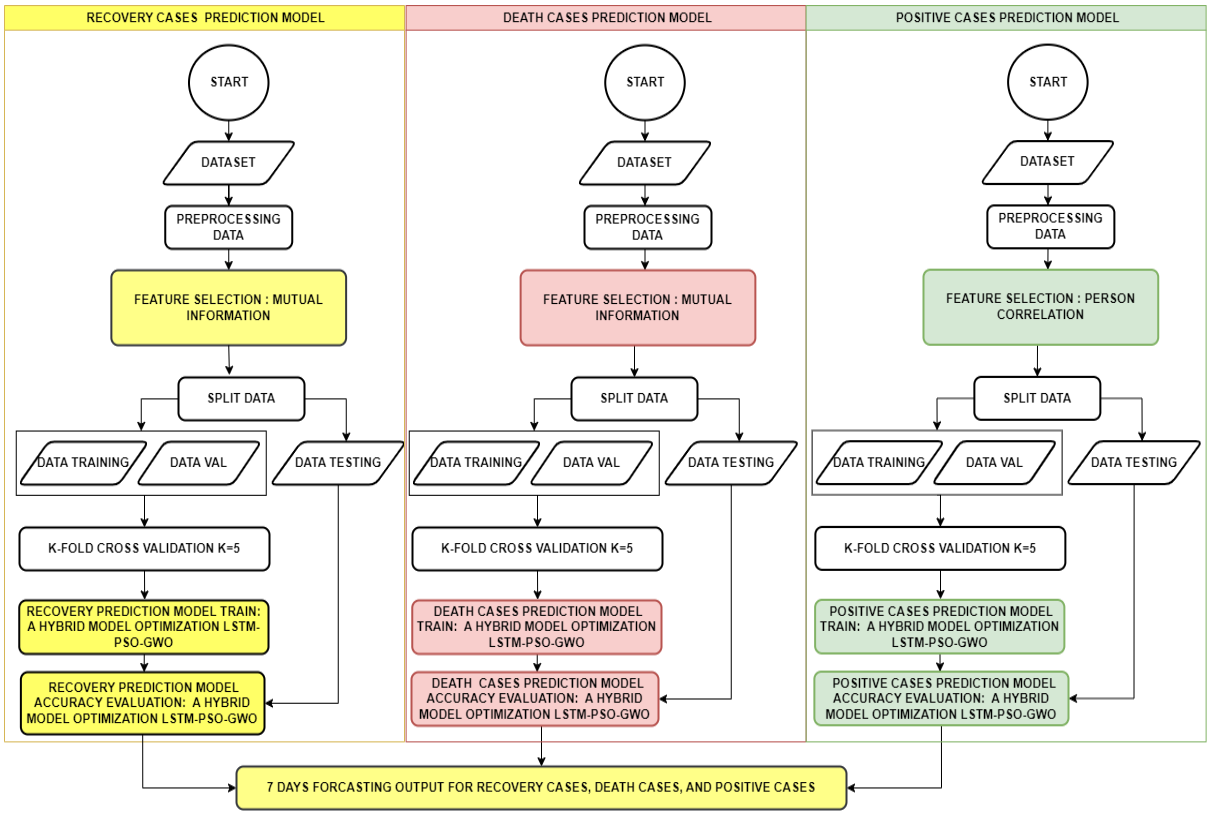

Figure 1. ADELMI framework: A Deep Learning and Metaheuristic Intelligence Framework for Short-Term Respiratory Virus Prediction

Vol. 7, No. 1, February 2026, Page. 373-390
https://jutif.if.unsoed.ac.id
DOI: https://doi.org/10.52436/1.jutif.2026.7.2.5485

2.1. Data Collection

The primary data source included in this research covering the period from March 2020 to December 2021 includes 657 daily records and 82 distinct variables. Epidemiological, testing, vaccination, and demographic data with 76 variables were obtained from the Layanan Permintaan Data, Ministry of Health of Indonesia (https://layanandata.kemkes.go.id/). Meteorological with 7 variables were collected from the Badan Meteorologi, Klimatologi, dan Geofisika (BMKG) (https://data.bmkg.go.id/), including: temperature max, avg temperature, humidity, rainfall, sun exposure, max wind speed, avg wind speed and merged using date alignment. All data were accessed from official and ethically compliant public sources.

Although the dataset spans 2020 to 2021, and the substantial variability of epidemic waves during this period provides rich temporal patterns that remain relevant for current endemic-phase surveillance and future respiratory virus spread. Core determinants of transmission, including testing intensity, vaccination progression, population activity, and meteorological conditions, have shown consistent influence on SARS-CoV-2 dynamics across different years and stages of circulation [48], [49].

2.2. Preprocessing

The step involved focusing on handling missing values using two techniques, namely mode replacement and zero replacement. Both techniques were employed to fill in the data gaps, thereby making the dataset more complete. Subsequently, variable scaling adjustments were made using the Rational Scale and Percentage Scale technique to ensure consistency in the analysis. Consequently, implementing the StandardScaler method followed the application of the Rational Scale and the Percentage Scale. The StandardScaler method was crucial in standardizing the data into a standard normal distribution with a mean of approximately 0 and a standard deviation of around 1.

2.3. Feature Selection

Feature selection was performed to identify the most relevant variables for each prediction target and to reduce redundancy within the heterogeneous multivariate dataset. Two complementary techniques were employed: Mutual Information (MI) and Pearson Correlation Coefficient (PCC).

The mutual_info_regression function from the scikit-learn library was utilized to compute the MI value. Iterations were performed through each additional feature against each target variable, and the results were stored as feature-value pairs of MI. The feature selection results were then sorted based on decreasing MI values. Features with higher MI values were considered more informative and were selected for inclusion in the recovery and mortality prediction models.

A correlation analysis using the Pearson correlation coefficient (PCC) was conducted to evaluate the association of 'Positive'. This research implemented a correlation threshold of 0.80 to ensure that only features demonstrating the highest degree of association with the target variable were utilized in model construction.

2.4. Data Splitting and K-fold Validation

In order to verify the validity and accuracy of the SAR-COV-2 prediction model under development, the procedure of data separation was conducted on two separate occasions. The initial dataset, consisting of 657 records, was partitioned into a training set including 80% of the data (526 records) and a testing set containing the remaining 20% (131 records). Subsequently, a second partition was conducted utilizing the K-Fold Cross Validation (K-Fold CV) technique on the training subset derived from the initial partition, yielding a total of 526 data.

In a K-Fold CV procedure with K=5, each fold is assigned 421 records (80%) of the training subset and 105 records (20%) of the validation set. The data was randomly distributed to guarantee

Vol. 7, No. 1, February 2026, Page. 373-390
https://jutif.if.unsoed.ac.id
DOI: https://doi.org/10.52436/1.jutif.2026.7.2.5485

impartiality in the examination. By thoroughly testing and validating the model, the reliability of predictions is increased.

Following the determination of the optimal fold value, a conclusive assessment was conducted on the most favorable fold model by subjecting it to testing using previously unseen data, specifically a test dataset consisting of 131 records. This is employed for the ultimate assessment to evaluate the model's efficacy in real-life scenarios.

2.5. Hybrid Modelling

In modeling process, the architecture of the LSTM model was initially constructed. The decision to employ LSTM was based on its ability to handle sequential data, in line with the evolving dynamics of SARS-CoV-2 spread over time. To address the weaknesses of LSTM that may affect prediction accuracy, hybrid parameter optimization was conducted through a combination of Particle Swarm Optimization (PSO) and Gray Wolf Optimization (GWO) approaches.

The optimization process of the hyrbid LSTM optimization with PSO-GWO model architecture in Figure 2 began with the definition of the function, 'calculate_fitness', which evaluated the loss value of the LSTM model based on a specific set of weights. The architecture of the LSTM layer was configured with 50 units, and 100 units hidden upon the features extracted by the previous layer, allowing the model to capture more complex patterns in the data. The model was then compiled using the Adam optimizer, a standard optimization algorithm for LSTM.

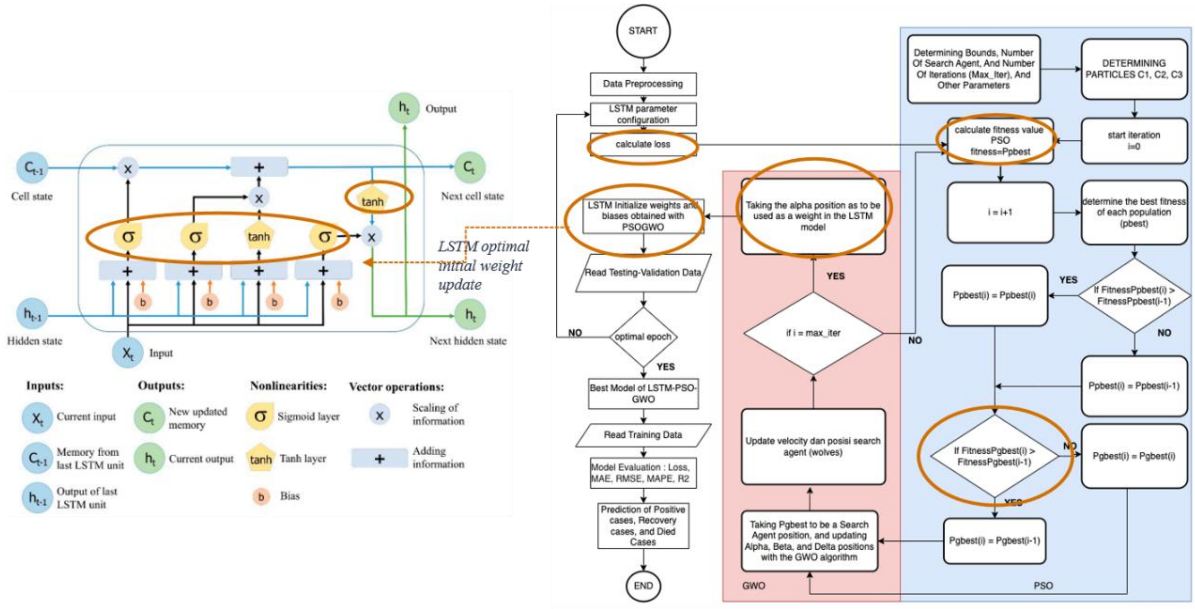

Figure 2. A Hybrid LSTM optimization with PSO-GWO model pipeline

The Particle Swarm Optimization (PSO) algorithm was then employed. This involved initializing a swarm of particles with random positions and velocities in a specific search space. The fitness of each particle was calculated using the 'calculate_fitness' function, and the best position (pbest) [50] for each particle as well as the global best position (gbest) were iteratively updated [51]. The PSO algorithm aimed to search for an optimal set of weights that minimized the loss function for the LSTM model.

Subsequently, the Gray Wolf Optimization (GWO) algorithm was applied. This algorithm simulated the social hierarchy and hunting behavior of gray wolves [52]. The positions of alpha, beta, and delta wolves were initialized, and their fitness values were evaluated. The alpha, beta, and delta wolves were updated based on their fitness values and dynamic parameters [53].

Vol. 7, No. 1, February 2026, Page. 373-390
https://jutif.if.unsoed.ac.id
DOI: https://doi.org/10.52436/1.jutif.2026.7.2.5485

In the hybrid optimization process, several important parameter values were set. Firstly, num_particles were configured to 50, determining the number of particles in the Particle Swarm Optimization (PSO) algorithm. These particles represented potential solutions in the search space, influencing the extent to which solutions were explored by the algorithm. Subsequently, num_dimensions, representing the number of parameters or weights in the LSTM model, was derived from the total number of parameters in the model. The search space, adjusted via search_space, determined the range of values allowed for each weight in the model, selected based on knowledge of the problem being addressed and data characteristics. A significant number of iterations, totaling 80,000, was designated for the PSO algorithm with num_iterations_pso, affecting how long the algorithm would run before producing the best solution. Furthermore, num_wolves_gwo was set to 50, determining the number of wolves in the Gray Wolf Optimization (GWO) algorithm, while num_iterations_gwo, also with a total of 80,000 iterations, influenced how long the GWO algorithm would run before producing the best solution. With the selection of these parameters, the goal was to achieve a balance between the quality of the solutions produced. The pseudocode for the hybrid LSTM-PSO-GWO model is in Figure 3.

```
Algorithm 1 Hybrid PSO–GWO Optimization for LSTM Parameters

Input:
  N – population size
  T – maximum iterations
  θ – initial LSTM parameter set
Output:
  θ* – optimized LSTM parameters

Initialize population Xi (i = 1...N) with random θ
Evaluate fitness f(Xi) using LSTM validation loss
Identify α, β, γ as the best three solutions
for t = 1 to T do
   # PSO update
   for each particle i do
      vi ← w·vi + c1·r1·(pbest_i – Xi) + c2·r2·(gbest – Xi)
      Xi_PSO ← Xi + vi
   end for
   # GWO update
   for each wolf i do
      Da ← |A1·Xα – Xi| ; Db ← |A2·Xβ – Xi| ; Dg ← |A3·Xγ – Xi|
      X1 ← Xα – C1·Da
      X2 ← Xβ – C2·Db
      X3 ← Xγ – C3·Dg
      Xi_GWO ← (X1 + X2 + X3) / 3
   end for
   # Hybrid exploitation–exploration fusion
   Xi_hybrid ← (Xi_PSO + Xi_GWO) / 2
   # Fitness evaluation
   Evaluate f(Xi_hybrid)
   Update pbest_i, α, β, γ
end for
return θ* = Xα
```

Figure 3. A Hybrid LSTM optimization with PSO-GWO Psoudocode

2.6. Model Training, Testing, and Validation

The training of the framework involves an iterative process in which the model is gradually adjusted to the training data to enhance its performance [54].. The training phase in this research was conducted by executing two datasets, namely the training and validation data, on the hybrid model that had been developed. The training aims to instruct the model on understanding the existing patterns within the data, thus enabling it to provide accurate predictions [7]. Simultaneously, the validation process was carried out using the validation dataset to evaluate the model's performance at each training iteration [8]. This ensures that the model not only learns the training data effectively but also can provide generalized predictions on unseen data [9].

The K-fold Cross Validation methodology was employed to partition the dataset into five subsets, which are subsequently employed for Training-Validation and Data Testing purposes. The K-Fold Training-Validation subset will be subjected to a training and testing procedure using the first model, which is a hybrid model incorporating LSTM-PSO-GWO optimization.

Vol. 7, No. 1, February 2026, Page. 373-390
https://jutif.if.unsoed.ac.id
DOI: https://doi.org/10.52436/1.jutif.2026.7.2.5485

2.7. Model Evaluation

The model evaluation used several metrics, including loss, root mean square error (RMSE), mean absolute percentage error (MAPE), and mean absolute error (MAE). These metrics employed to evaluate the accuracy of the model and comparing our proposed framework with previous models. Comparing model conducted to demonstrate that the newly proposed approach brings innovation with a significant improvement in accuracy against previous models, such as Single Linear Regression, MLP, LSTM, LSTM-PSO, and the SIR method.

3. RESULT

3.1. Preprocessing

3.1.1. Feature Scaling

The results of feature scaling on 82 variables, 62 variables were applied with the Rational Scale, and 20 variables were applied with the Percentage Scale. The final results of this feature scaling can be seen in Table 1, which shows the distribution of each feature according to the scale used.

Table 1. Feature Scaling

Scale	Features
Rational scale	'Daily cases', 'Imported cases', 'Local cases', 'Total cases', 'Active cases', 'Recovered (new)', 'Recovered', 'Dead (new)', 'Died', 'PDP , 'ODP', 'Active suspect', 'Number of specimens examined (from April 1)', 'Number of people examined', 'Negative', 'Positive (=C)', 'In Process', 'Specimen', 'Specimen (PCR-TCM)', 'Specimen (Antigen)', 'Tested person', 'Tested person (PCR-TCM)', 'Person those tested (Antigen)', 'Vaccination (ineligible)', 'Number of tests/million population', 'Test/Positive', 'Number of people tested/'positive', 'Number of daily Tests/Positives', 'Number of specimens examined (average 7 days)', 'Number of people examined (average 7 days)', 'Ratio of specimens/person examined (average 7 days)', 'First dose', 'Second dose', 'Third dose ', 'First dose (daily)', 'Second dose (daily)', 'Daily dose', 'First dose (weekly)', 'Second dose (weekly)', 'Average daily dose (weekly)', 'Dosage first (health human resources)', 'First dose (public workers)', 'Second dose (public workers)', 'Second dose (public workers) %', 'First dose (elderly)', 'First dose (general citizens) ', 'Second dose (general population)', 'First dose (adolescents)', 'Second dose (adolescents)', 'First dose (Vakgor)', 'Second dose (Vakgor)', 'National People PCR Test Average 7 day average', 'National Post Rate - 7 day average', 'Min Temperature', 'Max Temperature', 'AVg Temperature', 'HumidityAvg', 'Rainfall', 'Sun Explosure', 'Maximum wind speed' , 'Average wind speed'
Percentage Scale	'% active cases', 'Recovery rate (all cases)', 'Recovery rate (close cases)', 'Death rate (all cases)', 'Death rate (closed cases)', 'Positives / Number of Tests', 'Daily positive rate', 'Case Growth Rate ', 'Weekly positivity rate', 'First dose (%)', 'Second dose (%)', 'First dose (health HR) %', 'Second dose (health HR) %', 'First dose (public worker)) %', 'Second dose (public servants) %', First dose (elderly) %', 'Second dose (elderly) %',

3.1.2. StandarScaler Transformation

The results of the StandardScaler transformation on the SARS-CoV-2 dataset in Table 2 show that each feature, such as Daily Cases and Max Wind Speed, has been standardized to a z-score value.

Vol. 7, No. 1, February 2026, Page. 373-390
https://jutif.if.unsoed.ac.id
DOI: https://doi.org/10.52436/1.jutif.2026.7.2.5485

For example, on March 20, 2020, Daily Cases has a value of -0.0683310, meaning it is slightly lower than the average, while Max Wind Speed on the same date has a value of -0.995526, indicating a value significantly lower than the average. This process rescales the features to make them more homogeneous, making it easier for the model to learn data patterns effectively.

Table 2. The post-scaling transformations of SARS-CoV-2 Dataset

Date	Daily Cases	Imported Cases	Local Cases	….	Max Wind Speed	Avg Wind Speed
20-03-02	-.0683310	-0.058665	6.920967	….	-0.995526	1.883727
20-03-03	-.0683521	-0.058665	-0.74533	….	-0.358454	0.785538
20-03-04	-0.683521	-0.058665	-0.74533	….	1.977477	0.803395
…	…	…	…	…	…	…
21-12-19	-0,666235	-0.058665	-0.74533	….	4111619.0	0.172457

3.2. Feature Selection

The outcomes of feature selection process utilizing the MI method indicated that out of 83 features in the SARS-CoV-2 dataset in Indonesia, 20 features were chosen for the 'Recovered' target variable, and 20 features were selected for the 'Deceased' variable. Thus, the feature selection results reduced the dimensionality by 76% for death and recovery prediction.

Furthermore, an extra feature was obtained for the 'Positive' target through PCC feature selection. The outputs of feature selection can be observed in Table 3.

Table 3. Feature Selection for Recovery, Death, and Positive

Features Target	Technique	Features Selection
Recovery	MI	'Total cases', 'Deaths', 'Number of people tested', 'Number of specimens checked (from April 1)', 'Negative', 'Specimens', 'People tested', 'People tested (Antigen)', ' Number of tests/million population', 'Number of specimens examined (average 7 days)', 'Number of people examined (average 7 days)', 'First dose', 'Second dose', 'First dose (%)' , 'Second dose (%)', 'Second dose (daily)', 'Daily dose', 'First dose (weekly)', 'Second dose (weekly)', 'Average daily dose (weekly)'.
Death	MI	'Recovered', 'Total cases', 'Number of people tested', 'Number of specimens checked (from April 1)', 'Negative', 'Specimens', 'People tested', 'People tested (Antigen)', ' Number of tests/million population', 'Number of specimens examined (average 7 days)', 'Number of people examined (average 7 days)', 'First dose', 'Second dose', 'First dose (%)', 'Second dose (%)', 'Second dose (daily)', 'Daily dose', 'First dose (weekly)', 'Second dose (weekly)', 'Average daily dose (weekly)'
Positive	PCC	'The recovery rate (closed cases)'

3.3. Hybrid Deep Learning Metaheuristics Intelligence: Training, Testing, and Validation

3.3.1. Training and Testing

The training and testing results of the proposed Deep Learning and Metaheuristic Intelligence Framework are summarized in Table 3, encompassing hybrid LSTM–PSO–GWO models for recovery, death, and positive case forecasting. Feature selection was conducted using Mutual Information (MI)

Vol. 7, No. 1, February 2026, Page. 373-390
https://jutif.if.unsoed.ac.id
DOI: https://doi.org/10.52436/1.jutif.2026.7.2.5485

for recovery and death targets, and Pearson Correlation (PC) for positive cases. The results for recovery forecasting indicate a consistent improvement in accuracy as the number of epochs increased. The training phase demonstrated a significant reduction in Mean Absolute Error (MAE) from 11,415 to 1,886.64 and Root Mean Square Error (RMSE) from 21,067.5 to 4,165.55. Correspondingly, the Mean Absolute Percentage Error (MAPE) decreased from 2.9% to 0.85%, while the Root Mean Square Percentage Error (RMSPE) declined from 2.56% to 0.51%. Similar improvements were observed during testing, where the model achieved an MAE of 1,631.39 and a MAPE of 2.61%, indicating convergence stability and robust generalization at epoch 25.

For death prediction, the hybrid LSTM–PSO–GWO–MI model exhibited gradual but steady convergence. The training errors dropped from 250.12 (MAE) and 439.91 (RMSE) at epoch 1 to 91.5 and 164.3 at epoch 33, respectively. MAPE also declined notably from 3.3% to 0.81%. Testing outcomes confirmed consistent behavior, with MAE and RMSE of 99.7 and 168.3, and a MAPE of 3.6%, demonstrating strong stability and reliability in the optimized model.

In the case of positive case prediction, convergence occurred more gradually due to higher feature variability within the dataset. Nonetheless, a clear downward trend was observed across all metrics. Training MAE decreased from 2,937.7 to 691.5 and MAPE from 7.32% to 1.63% by epoch 30. Testing results reflected similar consistency, yielding an MAE of 945.11 and MAPE of 3.6%.

Overall, Table 4 confirms that the hybrid LSTM–PSO–GWO models effectively minimized forecasting errors across all categories, validating the synergistic effect of deep learning and metaheuristic optimization. To ensure the robustness and generalization of these results, a K-Fold Cross-Validation (K = 5) procedure was subsequently employed. This evaluation aimed to further assess consistency across varying temporal partitions and mitigate potential bias, reinforcing the reliability of the proposed framework for short-term respiratory virus forecasting.

Table 4. Training-Testing Hybrid Deep Learning Metaheuristics Intelligence for Recovery, Death, and Positive

Forecasting	Model	Epoch	Training				Testing			
			MAE	RMSE	MAPE %	RMSPE %	MAE	RMSE	MAPE %	RMSPE %
Recovery	LSTM-PSO-GWO-MI	1	11415	21067.5	2.9	2.56	1932.6	4051.5	3.1	1.48
		10	136462	360479	9.7	43.78	3765.69	6354.86	2.7	2.32
		15	2409.85	5137.8	1.1	0.62	1667.89	3902.13	2.66	1.42
		20	2061.78	4477.7	0.9	0.54	1984.08	4005.3	2.65	1.46
		25	1886.64	4165.55	0.85	0.51	1631.39	4070.04	2.61	1.48
Death	LSTM-PSO-GWO-MI	1	250.12	439.91	3.3	1.55	237.91	349.03	6.07	3.69
		15	101.2	190.7	1.43	0.67	102.95	211.9	3.86	2.24
		23	91.47	164.2	1.06	0.58	109.3	180.4	3.57	1.91
		28	87.3	162.4	0.87	0.57	89.58	176.1	3.6	1.86
		33	91.5	164.3	0.81	0.58	99.7	168.3	3.6	1.78
Positive	LSTM-PSO-GWO-PCC	1	2937.7	10145.4	7.32	27.8	3399.2	12689	9.89	34.7
		7	8007.4	12834.2	16.2	35.1	6827.8	9743.2	15.16	26.7
		13	1547.3	7621.11	4.01	20.9	1827.8	5945	5.34	16.3
		19	1507.03	7590.96	3.2	20.8	1041.4	5502.7	3.4	15.1
		25	989.34	7658.96	2.2	21.0	1052.5	5548.7	3.8	15.2
		30	691.5	7285.08	1.63	19.9	945.11	5498.1	3.6	15.1

3.3.2. K-fold Validation

The results of Kfold forcasting target of recovery in the Table 5 reveals varying performance metrics across different folds in the. Fold 1, the model showed signs of overfitting, with the validation MAPE 6.26% higher than the training 4.70%, and the MAE and RMSE lower on the training data, indicating the model fit the training data better than the validation data. In Fold 2, the model underfitted, with the validation MAPE 5.62% higher than the training 3.41%, and the MAE and RMSE higher on

Vol. 7, No. 1, February 2026, Page. 373-390
https://jutif.if.unsoed.ac.id
DOI: https://doi.org/10.52436/1.jutif.2026.7.2.5485

the validation data, indicating the model failed to capture patterns well in both the training and validation data. In Fold 3, the model showed a good fit, with the validation MAPE 2.85% better than the training 3.46%, and the MAE and RMSE stable between the training and validation data, indicating optimal performance. Fold 4 showed the best performance with the validation MAPE 0.83% lower than the training 3.61%, and the MAE and RMSE also lower on the validation, indicating a good model fit. Fold 5 shows underfitting, with the validation MAPE 1.88% higher than the training 3.26%, and the MAE and RMSE higher in validation, indicating the model is less able to capture patterns in the validation data.

Kfold forecasting target of death results in the Table 5 reveals Fold 1 signs of overfitting, with the validation MAPE 2.89% higher than the training 2.08%, and lower MAE and RMSE on the training data, indicating the model fits the training data better than the validation data. In Fold 2, the model experiences underfitting, with the validation MAPE 1.08% lower than the training 2.14%, and higher MAE and RMSE on the validation data, indicating the model is less able to capture the pattern optimally. Folds 3-5 show a fit model, with the validation MAPE consistently lower than the training MAPE. Fold 4 recorded the best validation MAPE 1.29, as well as lower MAE and RMSE, making it the best performing fold among all folds..

KFold forecasting target death base on Table 5 reveals Fold 1 exhibited overfitting, with a validation MAPE 0.95% lower than the training MAPE of 1.41%, and lower MAE and RMSE on the validation data, indicating that the model overfits the training data. On Folds 2 and 3, the model demonstrated good fit, with validation MAPEs of 0.53% and 0.47%, respectively. The MAE and RMSE were also stable between the training and validation data, indicating the model was able to produce accurate and consistent predictions on the validation data. Fold 4 recorded the best validation MAPE of 0.42%, and lower MAE and RMSE on the validation data, making it the best-performing fold. Fold 5 exhibited underfitting, with a validation MAPE 3.60% higher than the training MAPE of 0.60%, and higher MAE and RMSE on the validation data, indicating the model failed to generalize to previously unseen data.

Table 5. K-fold Cross Validation K=5 Hybrid Deep Learning Metaheuristics Intelligence for Recovery, Death, and Positive

Forecasting Target	Model	Fold	Training			Validation		
			MAE	RMSE	MAPE %	MAE	RMSE	MAPE %
Recovery	LSTM-PSO-GWO-MI	1	2645.86	4058.78	4.70	1998.72	3264.19	6.26
		2	2343.54	3646.92	3.41	2416.84	3610.48	5.62
		3	1283.80	2577.60	3.46	1741.46	3644.67	2.85
		4	1403.12	3052.34	3.61	1039.39	1917.02	0.83
		5	1232.55	2658.41	3.26	1466.71	3273.84	1.88
Death	LSTM-PSO-GWO-MI	1	250.33	406.14	2.08	165.31	338.28	2.89
		2	184.74	314.82	2.14	162.95	286.02	1.08
		3	151.43	274.31	1.75	195.16	283.60	2.22
		4	137.64	248.58	1.84	110.85	185.08	1.29
		5	160.08	270.68	1.89	113.58	214.98	1.20
Positive	LSTM-PSO-GWO-PCC	1	598.55	7598.38	1.41	399.69	2062.78	0.95
		2	557.33	7614.73	1.20	188.65	309.90	0.53
		3	617.85	7592.21	1.36	239.98	325.11	0.47
		4	555.19	7631.64	1.22	168.00	315.59	0.42
		5	231.52	350.38	0.60	1846.14	15246.4	3.60

Vol. 7, No. 1, February 2026, Page. 373-390
https://jutif.if.unsoed.ac.id
DOI: https://doi.org/10.52436/1.jutif.2026.7.2.5485

3.4. Hybrid Model Evaluation

Following performance evaluation feature impacts conducted using the K-fold cross-validation method, the hybrid LSTM-PSO-GWO in this research was subsequently tested and compared with traditional models such as ARIMA, SIR, SIRD, MLP, and Gaussian Naive Bayes in predicting recovery, death, and positive SARS-COV-2 cases. The comparison results in Tables 6 to 8.

Performance evaluation feature impacts in table 6 show that the ARIMA model demonstrated relatively decent performance with an MAE of 63191 and an RMSE of 30050. However, its inability to handle dynamic features and the complexity of SAR-COV-2 data is evident from the high MAPE of 23% and RMSPE of 10.95%. The SIR model exhibited suboptimal performance, particularly with highly high MAE and RMSE values of 1372161.2 and 2012165, respectively. Several metrics, such as MAPE and RMSPE, could not be computed, indicating limitations in the model's ability to address recovery case fluctuations. While the SIRD model showed improvement over SIR, it still reported high MAE and RMSE values 1207635 and 185081. Similar constraints were observed where specific metrics could not be calculated (NaN), and RMSPE reached 67.44%. The LSTM-PSO-GWO model without K-Fold Cross-Validation demonstrated impressive performance with MAE at 7132.9 and RMSE at 8309.7. Incorporating Feature Selection techniques, such as Mutual Information, contributed to increased accuracy, with low MAPE and RMSPE values of 0.20% and 3.03%, signifying the model's precision in predictions. The LSTM-PSO-GWO model with K-Fold Cross-Validation (K=5) showed further accuracy improvement, yielding an MAE of 2508.4 and RMSE of 4517.6. Using K-Fold enhanced the validity of model estimates, resulting in remarkably low MAPE and RMSPE values of 0.1% and 2%.

Table 6. Performance evaluation feature impacts: traditional models versus Hybrid Deep Learning Metaheuristics Intelligence for recovery cases Prediction LSTM-PSO-GW-MI

Models	FS	Val	Test MAE	Test RMSE	Test MAPE %	RMSPE %
ARIMA	-	-	63191	30050	23	10.95
SIR	-	-	1372161.2	2012165	NaN	Inf
SIRD	-	-	1207635	185081	NaN	67.44
MLP	-	Non KFold	328532672	4295573	inf	Inf
Gaussian Naive Bayes	-	Non KFold	855801278	1239088	inf	Inf
LSTM	MI	Non KFold	16788.6	18342.7	6.12	6.68
LSTM-PSO-GWO	MI	Non KFold	7132.9	8309.7	2.7	3.03
LSTM-PSO-GWO	MI	Kfold K=5	2508.4	4517.6	0.1	2

Note: infinity = the value > 100%.

The Performance evaluation feature impacts of LSTM-PSO-GWO for death cases prediction models presents a similar pattern as shown in Table 7, The ARIMA model, assessed without K-Fold Cross-Validation, demonstrated a moderate level of accuracy. With a Test MAE of 2,123 and Test RMSE of 5,981, it achieved a relatively low Test MAPE of 1%, indicating precise predictions. However, the RMSE percentage was comparatively high at 63%. Unfortunately, the SIR model cannot provide death cases prediction predictive. Further details on the model's performance are unavailable from the presented table. The SIRD model, evaluated without K-Fold Cross-Validation, reported a Test MAE of 47,247 and Test RMSE of 69,445. However, the absence of computable metrics such as Test MAPE (NAN) and an infinite RMSE percentage (Inf) indicates limitations in assessing the accuracy of death predictions. In contrast, the LSTM-PSO-GWO model, incorporating Mutual Information (MI) for feature selection without K-Fold Cross-Validation, exhibited promising results. The MAE was 963.8, the RMSE was 989.9, and the Test MAPE percentage was 0.70%. However, the RMSE percentage was

Vol. 7, No. 1, February 2026, Page. 373-390
https://jutif.if.unsoed.ac.id
DOI: https://doi.org/10.52436/1.jutif.2026.7.2.5485

relatively high at 10%. Furthermore, the LSTM-PSO-GWO model showcased enhanced performance, utilizing K-Fold Cross-Validation (K=5) with MI feature selection. The Test MAE further reduced to 497.7, the Test RMSE to 537.9, and the Test MAPE percentage improved to 0.35%. The RMSE percentage also showed improvement, decreasing to 6%.

Table 7. Performance evaluation feature impacts: traditional models versus Hybrid Deep Learning Metaheuristics Intelligence for death cases Prediction LSTM-PSO-GW-MI

Models	FS	Val	Test MAE	Test RMSE	Test MAPE %	RMSPE %
ARIMA	-	-	2123	5981	1	63
SIR	-	-	-	-	-	-
SIRD	-	-	47247	69445	NAN	Inf
MLP	-	Non KFold	52120648	619448149	Inf	Inf
Gaussian Naive Bayes	-	Non KFold	91156868	119153868	Inf	Inf
LSTM	MI	Non KFold	636406	667025	Inf	Inf
LSTM-PSO-GWO	MI	Non KFold	963.8	989.9	0.70	10
LSTM-PSO-GWO	MI	Kfold K=5	497.7	537.9	0.35	6

Note: infinity = the value > 100%.

Table 8. Performance evaluation feature impacts: traditional models versus Hybrid Deep Learning Metaheuristics Intelligence for positive cases prediction LSTM-PSO-GW-PCC

Models	FS	Val	Test MAE	Test RMSE	Test MAPE %	RMSPE %
ARIMA	-	-	12332	183.77	Inf	1.5
SIR	-	-	458479.2	631909.2	64.61	Inf
SIRD	-	-	32502	37485	71	Inf
MLP	-	Non KFold	33222970	41809862	Inf	Inf
Gaussian Naive Bayes	-	Non KFold	79599944	10915705	Inf	Inf
LSTM	PCC	Non KFold	45076	45076	Inf	Inf
LSTM-PSO-GWO	PCC	Non KFold	28.3	28.3	0.23	0.23
LSTM-PSO-GWO	PCC	Kfold K=5	25.36	25.36	0.05	0.21

Note: infinity = the value > 100%.

Tabel 8, provides a comprehensive comparison of performance evaluation feature impacts of LSTM-PSO-GWO for positive cases prediction model. The ARIMA model, evaluated without K-Fold Cross-Validation, demonstrated a Test MAE of 12,332 and an impressively low Test RMSE of 183.77. However, the Test MAPE was marked as infinite (Inf), suggesting challenges in accurately assessing the percentage error. The RMSE percentage was relatively small at 1.5%, indicating a comparatively low proportion of error. The SIR model, assessed without K-Fold Cross-Validation, presented a Test MAE of 458,479.2 and a substantial Test RMSE of 631,909.2. The Test MAPE percentage was notably high at 64.61%, indicating a significant percentage error. The RMSE percentage was marked as infinite (Inf), highlighting challenges in accurately assessing the error proportion. Similarly, the SIRD model, evaluated without K-Fold Cross-Validation, reported a Test MAE of 32,502 and a Test RMSE of 37,485. The Test MAPE percentage was notably high at 71%, indicating a substantial percentage error. Similar to SIR, the RMSE percentage was marked as infinite (Inf). On the other hand, the LSTM-PSO-GWO model, incorporating Pearson Correlation (PC) for feature selection without K-Fold Cross-Validation, demonstrated remarkable accuracy. Both Test MAE and Test RMSE were exceptionally low at 28.3.

Vol. 7, No. 1, February 2026, Page. 373-390
https://jutif.if.unsoed.ac.id
DOI: https://doi.org/10.52436/1.jutif.2026.7.2.5485

The Test MAPE percentage was minimal at 0.23%, indicating negligible percentage error. Impressively, s-PSO-GWO model, incorporating K-Fold Cross-Validation (K=5) with Pearson Correlation (PC) feature selection, continued to showcase high accuracy. Both Test MAE and Test RMSE were further reduced to 25.36. The Test MAPE percentage improved to 0.05%, indicating minimal percentage error. The RMSE percentage remained impressively low at 0.2%.

3.5. ADELMI Framework Forecasting Evaluation

The implementation of the ADELMI Framework for SARS-COV-2 Cases Spreading involved forecasting the number of recovery cases, deaths, and positive cases of SARS-COV-2 for a seven-day period. This decision was made because short-term projections are better suited to adapt to evolving circumstances, given the rapid fluctuations in pandemic dynamics and SARS-COV-2 -related factors. Although a 14-day timeframe can offer insights into longer-term trends, the heightened uncertainty and variability that typically arise over time can impact forecast accuracy.

The selection of a 7-day prediction window from August 21, 2021, to August 27, 2021, was motivated by an uptick in confirmed SARS-COV-2 cases despite widespread vaccination efforts. This increase was attributed to the emergence of three novel variants in August, namely SARS-CoV-2: Alpha, Beta, and Delta, which may have demonstrated heightened transmissibility or resistance to vaccines.

The assessment of the 7-day prediction framework yielded an accuracy in Table 9, which presented the percentage of prediction errors with MAPE and RMSPE for each model: Recovery Prediction, Death Prediction, and Positive Prediction. These findings indicate a positive assessment of the predictive accuracy achieved by the proposed framework: Deep Learning and Metaheuristic Intelligence Framework for Short-Term Respiratory Virus Prediction.

Table 9. The accuracy percentage of 7 days ADELMI prediction

Model	MAPE (%)	RMSPE (%)
Recovery Prediction	1.44	0.01
Death Prediction	3.00	0.05
Positive Prediction	0.01	0.05

The exceptional accuracy of the Recovery Prediction model is demonstrated by achieving a MAPE of 1.44% and a RMSPE of approximately 0.01, indicating that the recovery of SARS-COV-2 cases is predicted with a remarkably high level of accuracy. Figure 4, which depicts the plotline comparison between the original and forecasted data for SARS-CoV-2 recovery cases to bolster the conclusions.

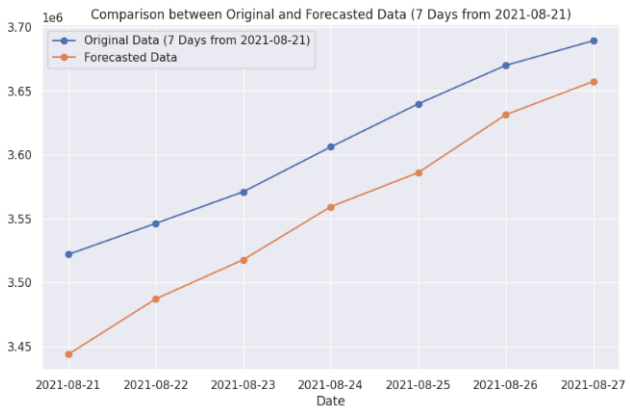

Figure 4. Comparison between original and forecasted data for SARS-CoV-2 recovery cases

Vol. 7, No. 1, February 2026, Page. 373-390
https://jutif.if.unsoed.ac.id
DOI: https://doi.org/10.52436/1.jutif.2026.7.2.5485

Similarly, the Death Prediction model exhibits a high level of accuracy, recording a MAPE of 3.00% and a RMSPE of 0.05%. Despite the MAPE and RMSPE exceeding the 10% criterion, they fall within the classification of "highly accurate forecasting," suggesting that mortality prediction attains a satisfactory level of precision. Figure 5, which depicts the plotline comparison between the original and forecasted data for SARS-CoV-2 death cases to bolster the conclusions.

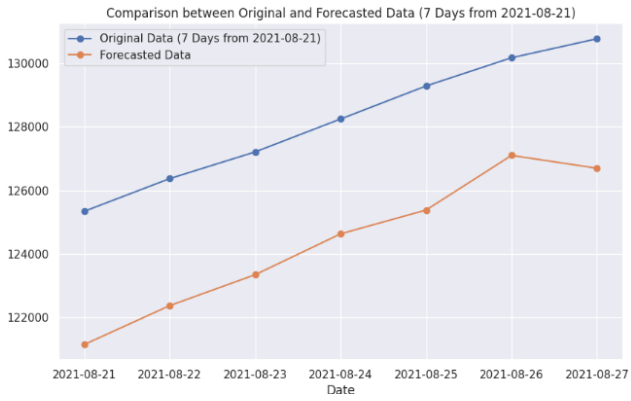

Figure 5. Comparison between original and forecasted data for SARS-CoV-2 death cases

The Positive Prediction model has attracted considerable attention owing to its exceptional accuracy, achieving a MAPE of 0.01% and an RMSPE of 0.05%. These values fall within the category of "Highly accurate forecasting," confirming that this model provides forecasts of positive SARS-COV-2 cases with an exceptionally high degree of accuracy. Figure 6, which depicts the plotline comparison between the original and forecasted data for SARS-CoV-2 death cases to bolster the conclusions.

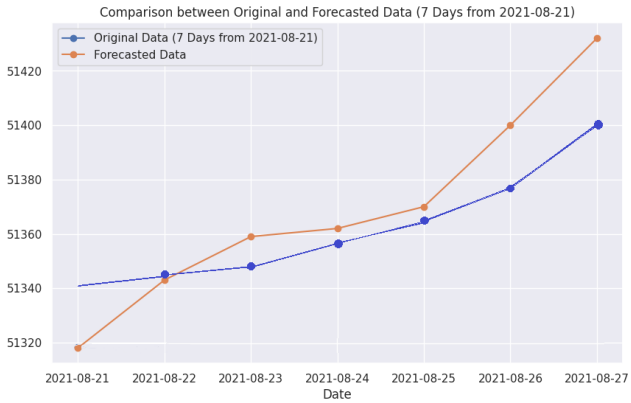

Figure 6. Comparison between original and forecasted data for SARS-CoV-2 positive cases

These findings provide compelling evidence for the reliability of ADELMI framwrok the 7-day prediction, instilling confidence in the models' precision in estimating SARS-COV-2 recoveries, death, and positive cases. This analysis further demonstrates the ADELMI capacity to identify and comprehend the evolving patterns of diseases and generate projections that are applicable to the current circumstances.

4. DISCUSSIONS

The main advantage of the ADELMI framework lies in its ability to process multivariate data. After feature selection, the model selects the most relevant features from the initial 82 variables, enabling it to more efficiently handle more complex data. Selected features, such as daily cases,

Vol. 7, No. 1, February 2026, Page. 373-390
https://jutif.if.unsoed.ac.id
DOI: https://doi.org/10.52436/1.jutif.2026.7.2.5485

vaccination rates, and meteorological variables, improve prediction accuracy.The hybrid model used in the ADELMI framework demonstrates superiority over previous researchers on hybrid models, such as MLP-ELM with a MAPE of 7.03% [55], XGBoost-SIRVD-LSTM with a MAPE of 0.9% and an RMSE of 35.025 [5], and GRU-LSTM with an RMSE of 69.92 [17].

5. CONCLUSION

By adopting a hybrid approach involving Mutual Information (MI) feature selection and Pearson correlation (PCC), integrated with the Particle Swarm Optimization (PSO) and Grey Wolf Optimizer (GWO) hybrid optimization algorithms in the Long Short-Term Memory (LSTM) structure, ADELMI framework succeeded in producing more accurate prediction models to handle heterogeneous-multivariate data. With MAPE and RMSPE scores consistently falling below the 10% threshold, highly accurate forecasting capabilities were demonstrated by ADELMI Framework. These results demonstrate the effectiveness of the unification of techniques in the hybrid model compared to previous methods. ADELMI supports the achievement of SDG 3 by providing adaptive and ethical forecasting solutions for global health, particularly in epidemiology and virus monitoring. ADELMI makes significant contributions to informatics by combining deep learning and metaheuristics, supporting SDG 9.

Moreover, potential future research could explore the utilization of the autoencoder technique to address missing values, offering an alternative approach to enhance the accuracy of the ADELMI framework. Through leveraging the autoencoder technique, the model could acquire more intricate and comprehensive data representations, potentially leading to improved accuracy in predicting suspected cases.

CONFLICT OF INTEREST

The authors declares that there is no conflict of interest between the authors or with research object in this paper.

ACKNOWLEDGEMENT

Authors acknowledge the support of Universitas Duta Bangsa Surakarta through the International Collaborative Research Grant 2025 (Grant No. 046/UDB.LPPM/A.34-SK/IX/2025) in partnership with Universiti Kuala Lumpur, and thank the Ministry of Health of the Republic of Indonesia and BMKG for providing the data used in this research.

REFERENCES

[1] R. Sk Abd Razak, A. Ismail, A. F. Abdul Aziz, L. S. Suddin, A. Azzeri, and N. I. Sha'ari, "Post-COVID syndrome prevalence: a systematic review and meta-analysis," BMC Public Health, vol. 24, no. 1, p. 1785, 2024, doi: 10.1186/s12889-024-19264-5.

[2] Z. Liu et al., "Modeling the trend of coronavirus disease 2019 and restoration of operational capability of metropolitan medical service in China: a machine learning and mathematical model-based analysis," Glob Health Res Policy, vol. 5, no. 1, 2020, doi: 10.1186/s41256-020-00145-4.

[3] M. U. G. Kraemer et al., "Artificial intelligence for modelling infectious disease epidemics," Nature, vol. 638, no. 8051, pp. 623–635, Feb. 2025, doi: 10.1038/s41586-024-08564-w.

[4] A. Haque and A. B. Pant, "The coevolution of Covid-19 and host immunity," Explor Med, vol. 5, no. 2, pp. 167–184, 2024, doi: 10.37349/emed.2024.00214.

[5] H. Alkhalefah, D. Preethi, N. Khare, M. H. Abidi, and U. Umer, "Deep learning infused SIRVD model for COVID-19 prediction: XGBoost-SIRVD-LSTM approach," Front Med (Lausanne), vol. 11, Sep. 2024, doi: 10.3389/fmed.2024.1427239.

[6] S. Y. Ilu and R. Prasad, "Time series analysis and prediction of COVID-19 patients using discrete wavelet transform and auto-regressive integrated moving average model," Multimed Tools Appl,

Vol. 7, No. 1, February 2026, Page. 373-390
https://jutif.if.unsoed.ac.id
DOI: https://doi.org/10.52436/1.jutif.2026.7.2.5485

vol. 83, no. 29, pp. 72391–72409, Feb. 2024, doi: 10.1007/s11042-024-18528-x.

[7] J. Farooq and M. A. Bazaz, "A deep learning algorithm for modeling and forecasting of COVID-19 in five worst affected states of India," Alexandria Engineering Journal, vol. 60, no. 1, pp. 587–596, Feb. 2021, doi: 10.1016/j.aej.2020.09.037.

[8] B. N. Harapan, T. Harapan, L. Theodora, and N. A. Anantama, "From Archipelago to Pandemic Battleground: Unveiling Indonesia's COVID-19 Crisis," J Epidemiol Glob Health, vol. 13, no. 4, pp. 591–603, Sep. 2023, doi: 10.1007/s44197-023-00148-7.

[9] M. Khairulbahri, "Lessons learned from three Southeast Asian countries during the COVID-19 pandemic," J Policy Model, vol. 43, no. 6, pp. 1354–1364, Nov. 2021, doi: 10.1016/j.jpolmod.2021.09.002.

[10] C. B. Aditya Satrio, W. Darmawan, B. U. Nadia, and N. Hanafiah, "Time series analysis and forecasting of coronavirus disease in Indonesia using ARIMA model and PROPHET," Procedia Comput Sci, vol. 179, pp. 524–532, 2021, doi: 10.1016/j.procs.2021.01.036.

[11] B. A. Wahyudi and I. Palupi, "Prediction of the peak Covid-19 pandemic in Indonesia using SIR model," Jurnal Teknologi dan Sistem Komputer, vol. 9, no. 1, pp. 49–55, 2021, doi: 10.14710/jtsiskom.2020.13877.

[12] K. S. Reddy, "Prediction of covid-19 outbreak in India by employing epidemiological models," Journal of Computer Science, vol. 16, no. 7, pp. 886–890, 2020, doi: 10.3844/jcssp.2020.886.890.

[13] O. Melikechi, A. L. Young, T. Tang, T. Bowman, D. Dunson, and J. Johndrow, "Limits of epidemic prediction using SIR models," J Math Biol, vol. 85, no. 4, pp. 1–29, 2022, doi: 10.1007/s00285-022-01804-5.

[14] J. Milojković, M. Milić, and V. Litovski, "ANN model for one day ahead Covid-19 prediction," in International Conference IcETRAN, etran.rs, 2022, pp. 1–4. doi: 10.1016/S1044-5803(96)00098-8.

[15] A. N. Akramin Kamarudin, Z. Zainol, N. F. Abu Kassim, and R. Sharif, "Prediction of COVID-19 Cases in Malaysia by Using Machine Learning: A Preliminary Testing," in 2021 International Conference of Women in Data Science at Taif University (WiDSTaif), IEEE, Mar. 2021, pp. 1–6. doi: 10.1109/WiDSTaif52235.2021.9430222.

[16] K. Ganesh and B. Vani, "An Efficient COVID-19 Pandemic Survival Analysis to Compare Random Forest and Support Vector Machine for Classifying Performance in Censored Data," ECS Trans, vol. 1, no. 107, p. 12993, 2022, doi: 10.1149/10701.12993ecst.

[17] S. Prakash, A. S. Jalal, and P. Pathak, "Forecasting COVID-19 Pandemic using Prophet, LSTM, hybrid GRU-LSTM, CNN-LSTM, Bi-LSTM and Stacked-LSTM for India," in 2023 6th International Conference on Information Systems and Computer Networks (ISCON), IEEE, Mar. 2023, pp. 1–6. doi: 10.1109/ISCON57294.2023.10112065.

[18] S. Sanche, Y. T. Lin, C. Xu, E. Romero-Severson, N. Hengartner, and R. Ke, "High Contagiousness and Rapid Spread of Severe Acute Respiratory Syndrome Coronavirus 2," Emerg Infect Dis, vol. 26, no. 7, pp. 1470–1477, 2020, doi: 10.3201/eid2607.200282.

[19] C. Yu et al., "Clinical Characteristics, Associated Factors, and Predicting COVID-19 Mortality Risk: A Retrospective Study in Wuhan, China," Am J Prev Med, vol. 59, no. 2, pp. 168–175, 2020, doi: 10.1016/j.amepre.2020.05.002.

[20] S. Chen, R. Paul, D. Janies, K. Murphy, T. Feng, and J. C. Thill, "Exploring Feasibility of Multivariate Deep Learning Models in Predicting COVID-19 Epidemic," Front Public Health, vol. 9, no. July, pp. 1–6, 2021, doi: 10.3389/fpubh.2021.661615.

[21] J. Kim and O. Kwon, "A model for rapid selection and covid-19 prediction with dynamic and imbalanced data," Sustainability (Switzerland), vol. 13, no. 6, pp. 1–18, 2021, doi: 10.3390/su13063099.

[22] A. Deniz, H. E. Kiziloz, E. Sevinc, and T. Dokeroglu, "Predicting the severity of COVID-19 patients using a multi-threaded evolutionary feature selection algorithm," Expert Syst, vol. 39, no. 5, pp. 1–11, 2022, doi: 10.1111/exsy.12949.

[23] P. Wendland et al., "Machine learning models for predicting severe COVID-19 outcomes in hospitals," Inform Med Unlocked, vol. 37, no. November 2022, 2023, doi: 10.1016/j.imu.2023.101188.

[24] H. Chauhan, K. Modi, and S. Shrivastava, "Development of a classifier with analysis of feature selection methods for COVID-19 diagnosis," World Journal of Engineering, vol. 19, no. 1, pp. 49–57, Jan. 2022, doi: 10.1108/WJE-10-2020-0537.
[25] J. Ircio, A. Lojo, U. Mori, and J. A. Lozano, "Mutual information based feature subset selection in multivariate time series classification," Pattern Recognit, vol. 108, 2020, doi: 10.1016/j.patcog.2020.107525.
[26] F. M. Khan and R. Gupta, "ARIMA and NAR based prediction model for time series analysis of COVID-19 cases in India," Journal of Safety Science and Resilience, vol. 1, no. 1, pp. 12–18, 2020, doi: 10.1016/j.jnlssr.2020.06.007.
[27] N. Ayoobi et al., "Time series forecasting of new cases and new deaths rate for COVID-19 using deep learning methods," Results Phys, vol. 27, no. June, 2021, doi: 10.1016/j.rinp.2021.104495.
[28] A. Barman, "Time Series Analysis and Forecasting of COVID-19 Cases Using LSTM and ARIMA Models," arXiv e-prints, vol. 1, no. 2006, p. 13852, 2020, doi: 10.48550/arXiv.2006.13852.
[29] A. Swaraj, A. Kaur, K. Verma, G. Singh, A. Kumar, and ..., "Implementation of Stacking Based ARIMA Model for Prediction of Covid-19 Cases in India," 2020, researchsquare.com. [Online]. Available: https://www.researchsquare.com/article/rs-52063/latest.pdf
[30] Magesh S, Niveditha V.R, Rajakumar P.S, Radha RamMohan S, and Natrayan L., "Pervasive computing in the context of COVID-19 prediction with AI-based algorithms," International Journal of Pervasive Computing and Communications, vol. 16, no. 5, pp. 477–487, Aug. 2020, doi: 10.1108/IJPCC-07-2020-0082.
[31] A. Zeroual, F. Harrou, A. Dairi, and Y. Sun, "Chaos , Solitons and Fractals Deep learning methods for forecasting COVID-19 time-Series data : A Comparative study," Chaos, Solitons and Fractals: the interdisciplinary journal of Nonlinear Science, and Nonequilibrium and Complex Phenomena, vol. 140, p. 110121, 2020, doi: 10.1016/j.chaos.2020.110121.
[32] S. D. Khan, L. Alarabi, and S. Basalamah, "Toward smart lockdown: A novel approach for covid-19 hotspots prediction using a deep hybrid neural network," Computers, vol. 9, no. 4, pp. 1–16, 2020, doi: 10.3390/computers9040099.
[33] H. Abbasimehr and R. Paki, "Prediction of COVID-19 confirmed cases combining deep learning methods and Bayesian optimization," Chaos Solitons Fractals, vol. 142, p. 110511, 2021, doi: 10.1016/j.chaos.2020.110511.
[34] Y. Hao, T. Xu, H. Hu, P. Wang, and Y. Bai, "Prediction and analysis of Corona virus disease 2019," PLoS One, vol. 15, no. 10 October, 2020, doi: 10.1371/journal.pone.0239960.
[35] M. O. Alassafi, M. Jarrah, and R. Alotaibi, "Time series predicting of COVID-19 based on deep learning," Neurocomputing, vol. 468, pp. 335–344, 2022, doi: 10.1016/j.neucom.2021.10.035.
[36] A. Pranolo, Y. Mao, A. P. Wibawa, A. B. P. Utama, and F. A. Dwiyanto, "Robust LSTM With Tuned-PSO and Bifold-Attention Mechanism for Analyzing Multivariate Time-Series," IEEE Access, vol. 10, no. July, pp. 78423–78434, 2022, doi: 10.1109/ACCESS.2022.3193643.
[37] W. Lu, W. Jiang, N. Zhang, and F. Xue, "Application of PSO-based LSTM Neural Network for Outpatient Volume Prediction," J Healthc Eng, vol. 2021, p. 7246561, 2021, doi: 10.1155/2021/7246561.
[38] Y. Zhang and S. Yang, "Prediction on the highest price of the stock based on PSO-LSTM neural network," in 3rd International Conference on Electronic Information Technology and Computer Engineering, EITCE 2019, IEEE, 2019, pp. 1565–1569. doi: 10.1109/EITCE47263.2019.9094982.
[39] S. Prasanth, U. Singh, A. Kumar, V. Anand, and P. H. J. Chong, "Chaos , Solitons and Fractals Forecasting spread of COVID-19 using google trends : A hybrid GWO-deep learning approach R," Chaos, Solitons and Fractals: the interdisciplinary journal of Nonlinear Science, and Nonequilibrium and Complex Phenomena, vol. 142, p. 110336, 2021, doi: 10.1016/j.chaos.2020.110336.
[40] C. Li and R. Lu, "Short-term power forecasting model based on GWO-LSTM network," J Phys Conf Ser, vol. 2503, no. 1, pp. 0–8, 2023, doi: 10.1088/1742-6596/2503/1/012039.
[41] G. Shial, S. Sahoo, and S. Panigrahi, An Enhanced GWO Algorithm with Improved Explorative Search Capability for Global Optimization and Data Clustering, vol. 37, no. 1. Taylor & Francis,

Vol. 7, No. 1, February 2026, Page. 373-390
https://jutif.if.unsoed.ac.id
DOI: https://doi.org/10.52436/1.jutif.2026.7.2.5485

2023. doi: 10.1080/08839514.2023.2166232.
[42] H. Ponce, "Optimization of the Containment Levels for the Reopening of Mexico City due to COVID-19," IEEE Latin America Transactions, 2020, [Online]. Available: https://latamt.ieeer9.org/index.php/transactions/article/view/4416
[43] A. Sîrbu et al., "Early outcome detection for COVID-19 patients," Sci Rep, vol. 11, no. 1, pp. 1–14, 2021, doi: 10.1038/s41598-021-97990-1.
[44] Y. Peng, C. Li, Y. Rong, C. P. Pang, X. Chen, and H. Chen, "Real-time prediction of the daily incidence of COVID-19 in 215 countries and territories using machine learning: Model development and validation," J Med Internet Res, vol. 23, no. 6, pp. 1–18, 2021, doi: 10.2196/24285.
[45] I. Riadi, R. Umar, and R. Anggara, "Comparative Analysis of Naive Bayes and K-Nearest Neighbor Approaches to Predict Timely Graduation using Academic History," International Journal of Computing and Digital Systems, vol. 15, pp. 2142–2210, May 2024, doi: 10.12785/ijcds/160185.
[46] A. Fadlil, I. Riadi, and F. Andrianto, "Improving Sentiment Analysis in Digital Marketplaces through SVM Kernel Fine-Tuning," International Journal of Computing and Digital Systems, vol. 15, pp. 159–171, Jul. 2024, doi: 10.12785/ijcds/160113.
[47] A. S. Abu-alhaija, "From Epistemology to Structural Equation Modeling: An Essential Guide in Understanding the Principles of Research Philosophy in Selecting the Appropriate Methodology," Aust J Basic Appl Sci, vol. 13, no. 9, 2019, doi: 10.22587/ajbas.2019.13.9.12.
[48] M. Posse et al., "Lessons learnt in the response to COVID-19 in Mozambique: enabling readiness for the next pandemic," Frontiers in Health Services, p., 2025, doi: 10.3389/frhs.2025.1612577.
[49] K. Matsumoto et al., "Uncertainty and decision-making in critical care: lessons from managing COVID-19 ARDS in preparation for the next pandemic," BMJ Open Respir Res, vol. 12, p., 2025, doi: 10.1136/bmjresp-2024-002637.
[50] S. Samsuddin, M. S. Othman, and L. M. Yusuf, "a Review of Single and Population-Based Metaheuristic Algorithms Solving Multi Depot Vehicle Routing Problem," International Journal of Software Engineering and Computer Systems, vol. 4, no. 2, pp. 80–93, 2018, doi: 10.15282/ijsecs.4.2.2018.6.0050.
[51] I. M. El-Hasnony, S. I. Barakat, and R. R. Mostafa, "Optimized ANFIS Model Using Hybrid Metaheuristic Algorithms for Parkinson's Disease Prediction in IoT Environment," IEEE Access, vol. 8, no. September, pp. 119252–119270, 2020, doi: 10.1109/ACCESS.2020.3005614.
[52] P. Kandasamy, "Literature Review on Grey Wolf Optimization Techniques," International Journal of Science and Research, vol. 9, no. 12, pp. 1765–1769, 2020, doi: 10.21275/SR20506165027.
[53] J. Aguila-Leon, C. Chiñas-Palacios, C. Vargas-Salgado, E. Hurtado-Perez, and E. X. M. Garcia, "Particle swarm optimization, genetic Algorithm and grey Wolf optimizer algorithms performance comparative for a DC-DC boost converter PID controller," Advances in Science, Technology and Engineering Systems, vol. 6, no. 1, pp. 619–625, 2021, doi: 10.25046/aj060167.
[54] Z. Guo, Q. Lin, and X. Meng, "A Comparative Study on Deep Learning Models for COVID-19 Forecast," Healthcare (Switzerland), vol. 11, no. 17, pp. 1–13, 2023, doi: 10.3390/healthcare11172400.
[55] R. P. Shetty and P. S. Pai, "Forecasting of COVID 19 Cases in Karnataka State using Artificial Neural Network (ANN)," Journal of The Institution of Engineers (India): Series B, vol. 102, no. 6, pp. 1201–1211, 2021, doi: 10.1007/s40031-021-00623-4.